Discrete functional motifs reside within the cytoplasmic tail of α_V integrin subunit

Thomas A. Haas

Department of Anatomy and Cell Biology and Molecular Design Research Group, College of Medicine, University of Saskatchewan, Saskatoon, Canada

Summary

Previous studies have demonstrated that cell-permeable cytoplasmic tail (CT) $\alpha_{II}\beta$ peptides can modulate the activation of $\alpha_{IIb}b_3$. As α_V CT contains an $\alpha_{II}\beta$ homologous region, a series of cell-permeable α_V and α_{IIb} peptides were generated to determine if α_V CT can modulate the activation of β_3 integrins in comparison to α_{IIb}, and to identify the minimal bioactive sequences in α_V CT. Using NMR structures and molecular models as guides, the initial peptides for study encompassed the $\alpha_{II}\beta$ homologous sequences of α_V CT (α_V(987–1006); V-1), its amino-terminus (α_V(987–993);V-2), a turn motif (α_V(993–1001);V-3), the carboxyl-terminus (α_V(999–1006); V-4), and corresponding homologous α_{IIb} peptides. Treatment of platelets and $\alpha_V\beta_3$-expressing cells with the peptides revealed that IIb-1 inhibited $\alpha_{IIb}\beta_3$ activation and V-1 inhibited $\alpha_V\beta_3$ activation, but not vice versa. The inhibitory capacity of these peptides was mapped to the central turn-motif region which was encompassed by V-3, but only partially by IIb-3. V-2 and IIb-2 activated both β_3 integrins, while V-4 and IIb-4 were inactive. The use of truncation and mutant peptides confirmed the importance of the turn motif for inhibitory activity and identified the side-chain of α_V(Q1001) as a critical inhibitory residue. The difference in the integrin inhibitory capacity of α_V and α_{IIb} peptides and their capacity to influence the assembly of kinases with integrin CTs, reveals a possible divergence in the regulatory control of the two β_3 integrins.

Keywords

GP IIb/IIIa, Integrins, antiplatelet agents, fibrinogen / fibrin

Thromb Haemost 2008; 99: 96–107

Introduction

Integrins are a family of cell receptors that mediate cell-cell and cell-substratum interactions (1). These basic biological events determine processes of development, haemostasis and thrombosis, inflammation, and tumor metastasis. A typical integrin consists of an α and a β subunit that are held together by numerous contacts and divalent cations. Each subunit is a type I transmembrane protein (1, 2). An important regulatory property of integrins is that high affinity ligand binding is usually not constitutive but requires a cellular activation-dependent process, entitled *inside-out* signaling or *affinity modulation* (3). While the precise details of *inside-out* signaling remain unknown, it is clear that integrin cytoplasmic tails (CTs) play a central and critical role in this process, transposing the signaling of intracellular pathways into a structural change within the extracellular domain of the integrin that permits effectual ligand binding (4, 5). The crystal structures of the extracellular domain of $\alpha_{IIb}\beta_3$ and $\alpha_V\beta_3$ have been solved with and without bound ligands (6–8). The structure folds into known and novel domains and comparison of the structures of $\alpha_V\beta_3$ and $\alpha_{IIb}\beta_3$ reveals the atomic basis for $\alpha_{IIb}\beta_3$ activation, the swing-out of the hybrid and PSI domains of β_3 (8). Mutational studies have since determined the functional significance of several residues within or near the RDG-binding site in the α_{IIb}, α_V, and β_3 subunits (9–12). Following the ligand binding to the extracellular domain of integrins, a variety of intracellular responses are elicited, including cytoskeleton reorganization, intracellular ion transport, kinase activation, and tyrosine phosphorylation (3, 13, 14).

The β_3 integrin family, $\alpha_{IIb}\beta_3$ and $\alpha_V\beta_3$, provides evidence for *inside-out* signaling, and for the importance of the CTs in regulating this process (4, 15, 16). The importance of rapid and regulated changes in integrin affinity is easily appreciated for $\alpha_{IIb}\beta_3$, as platelets must interact with fibrinogen (Fg) in a rapid manner only following vascular injury to maintain homeostasis. The significance of *inside-out* signaling for $\alpha_V\beta_3$ is also apparent in a

Correspondence to:
Thomas Haas
University of Saskatchewan
Rm A315 Health Sciences Building
107 Wiggins Road, Saskatoon,
SK, Canada S7N 5E5
Tel.: +1 306 966 8088, Fax: +1 306 966 4298
E-mail: thomas.haas@usask.ca

Financial support:
This work was supported by a Canadian Research Chair award, and Canadian Institutes of Health Research and Saskatchewan Health Research Foundation grants.

Received August 7, 2007
Accepted after major revision November 2, 2007

Prepublished online December 5, 2007
doi:10.1160/TH07–08–0498

number of cell types, where cell stimulation leads to an increase in $\alpha_V\beta_3$-mediated cell adhesion and soluble ligand binding (16, 17). Mutational studies implicate the involvement of both the α and β CTs in *inside-out* signaling with point mutations within the β_3 CT, preventing both $\alpha_V\beta_3$ and $\alpha_{IIb}\beta_3$ from becoming competent receptors, while deletion of the membrane-proximal region of either subunit results in the expression of a constitutively active receptor (4, 5, 15, 18). Truncations and mutations within the α CT also resulted in constitutive activation and/or inactivation of $\alpha_{IIb}\beta_3$ and $\alpha_V\beta_3$ (5, 15, 19, 20). Other studies suggest that the CTs may generate the *inside-out* signal as a result of a change in the α/β cytoplasmic interface (15, 21, 22). The existence and identity of the amino acids that comprise this interface were first determined using isolated α and β CTs and subsequently, the biological importance of one of these intra-subunit contacts was confirmed by point mutational analysis (15, 21–23). Nuclear magnetic resonance structures of the α_{IIb} CT reveal that its highly conserved amino (N) juxtatransmembrane region forms an α-helix, followed by a turn, and then its flexible acidic carboxyl (C) -terminus folds back onto the N-terminal helix (24). In addition, structural analysis of α_{IIb} CT and of the α/β cytoplasmic complex support the speculation of the α/β cytoplasmic interface playing a central regulatory role in *inside-out* signaling and identified additional intra-subunit contacts (24, 25).

The interaction of integrin β cytoplasmic domains with talin and other intracellular proteins are implicated in integrin activation, presumably by altering the structure of the a/b complex (25–30). A number of proteins are also reported to interact with the juxtatransmembrane region of integrin a CTs such as actin (31), talin (32), calcium-integrin binding protein 1 (CIB1) (33), ancient ubiquitous protein (34), current chloride nucleotide protein (35), and protein phosphatase 1 (36). However, with the exception of CIB1, the significance of these interactions in regulating integrin activation has not been resolved. The interaction of CIB1 with α CTs was shown to be specific for α_{IIb} as it did not interact with the α_v, α_2 or α_5 (31). More recently, CIB1 was identified as an endogenous inhibitor of $\alpha_{IIb}\beta_3$ activation by interfering with talin binding to the β_3 CT (37). Using a cell-permeable peptide approach, it was demonstrated that incubation of platelets with α_{IIb}(989–995), the juxtatransmembrane region of α_{IIb}, resulted in activation of $a_{IIb}b_3$ in an agonist-independent manner (38, 39), which is consistent with the role for this region in CIB1 binding and $\alpha_{IIb}\beta_3$ activation (18, 34, 40). However, treatment with cell-permeable α_{IIb}(989–1008), resulted in the inhibition of agonist-induced $\alpha_{IIb}\beta_3$ activation (24), and a subsequent study further narrowed the region responsible for this inhibitory capacity (41). Thus, there is mounting evidence that there are a number of bioactive sequences present within the short CT of α_{IIb}. However, no studies have reported whether cell-permeable peptides derived from α_V exhibit similar functional capacity. Therefore, as the N-region of α_V CT [α_V(987–1006)] is homologous to the CT of α_{IIb}, experiments were performed to test whether the CT of α_V has similar biological properties.

In the present work, the capacity of cell-permeable α_V CT peptides to influence $\alpha_{IIb}\beta_3$ and $\alpha_V\beta_3$ activation was determined in parallel with control homologous α_{IIb} peptides. Treatment of platelets and $\alpha_V\beta_3$-expressing cells with α_{IIb}(989–1008) and α_V(987–1006) revealed that there is specificity in the capacity of these two peptides to inhibit β_3 integrin activation. Using a series of truncated CT peptides, α_V(993–1001) was identified as the minimal inhibitory sequence within α_V CT that inhibited β_3 activation, while its homologous α_{IIb} counterpart was inactive. Using additional truncated and mutant α_V(993–1001) peptides, α_V(Q1001) was identified as a critical residue for endowing inhibitory capacity to α_V(993–1001). As α_V(993–1001) prevented the dissociation of Csk from the CTs of $\alpha_{IIb}\beta_3$ and Src activation, the capacity of α_V(993–1001) to suppress integrin activation maybe linked to a disruption in kinase-integrin interactions. These findings support the hypothesis that the αCTs of integrins play a central role in regulating integrin activation and identify commonalities and differences in the mechanism by which β_3 integrin activation is regulated.

Materials and methods

Antibodies and reagents

PAC1 and FITC-labeled PAC1 were obtained from Becton Dickinson (Oakville, ON, Canada). LM609 and human vitronectin were obtained from Chemicon International (Billerica, MA, USA). AP3, talin and phospho-Src antibodies were obtained from GTI, Sigma and Cell Signaling (Waukesha, WI, USA; Danvers, MA, USA), respectively. All other kinase, integrin and anti-IgG antibodies were obtained from Santa Cruz Biotechnology (Santa Cruz, CA, USA). Human prothrombin was obtained Enzyme Research Laboratories (Swansea, UK). Fluorescence labeling reagents and anti-fluorescein antibodies were obtained from Molecular Probes (Burlington, ON, Canada). Laboratory chemicals were obtained from VWR International (Mississauga, ON, Canada). CM5 sensor chips were obtained from Biacore, and Super Signal and GelCode Blue were obtained from Pierce (Piscataway, NJ, USA and Rockford, IL, USA).

Cell culture and cytotoxicity assay

$\alpha_V\beta_3$-expressing cell lines, GM1500s, and bovine aortic endothelial cells (BAECs), were grown in DMEM F-12 media containing 10% FBS following standard procedures (16). Human platelets were prepared from peripheral venous blood of apparently healthy volunteers and isolated by gel filtration on Sepharose CL 2b as previously described (42). Cell and platelet concentrations were measured on a Z1 dual threshold coulter counter (Beckman Coulter, Fullerton, CA, USA). The cytotoxicity effects of the peptide treatment was evaluated using the colorimetric MTT assay kit from Chemicon (Billerica, MA, USA) following manufactures recommended procedures. Cells were plated onto 96 wells plates, treated with a number of the test peptides at a concentration of 100 μM, and then incubated for four hours at 37°C for MTT cleavage to occur. MTT cleavage was measured at 570 nm on a SpectraMax M2e microplate reader (Molecular Devices, Sunnyvale, CA, USA).

Protein isolation

Human talin was obtained from outdated platelets by a combination of ion-exchange and size-exclusion chromatography as previously described (43). The head domain of talin (talin-H) was obtained during talin purification or prepared by cleavage of

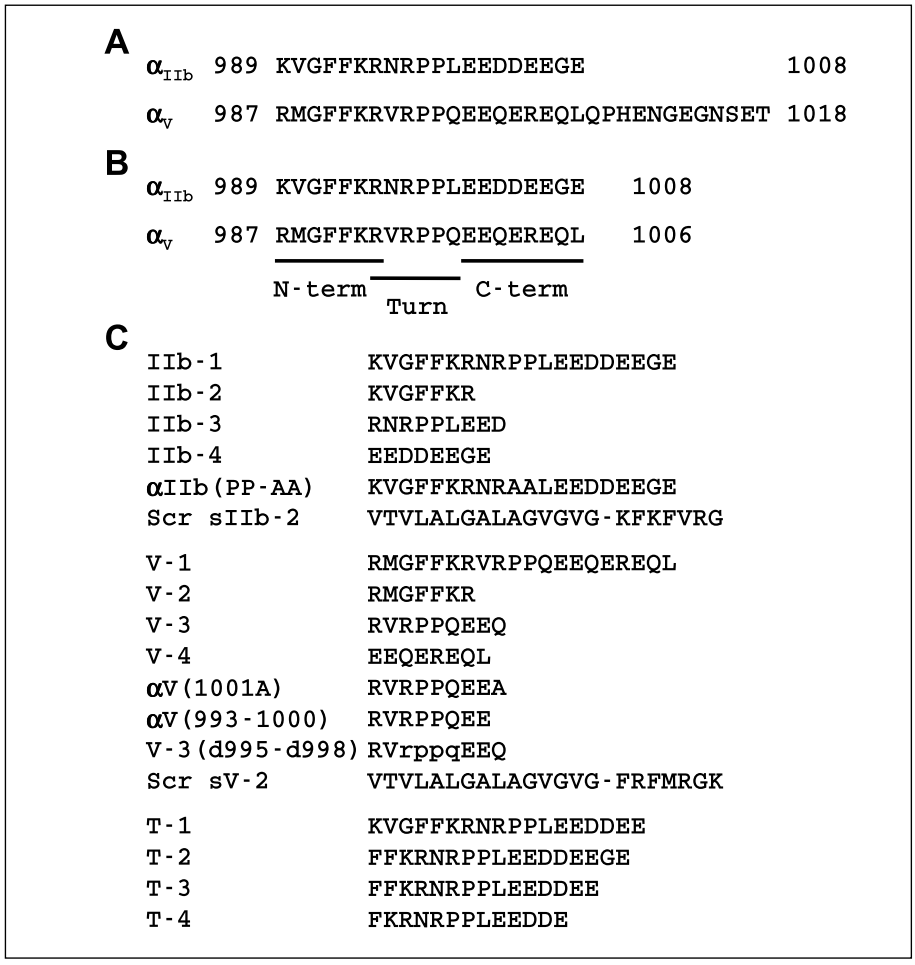

Figure 1: α CT peptide sequences. A) The sequence of the cytoplasmic domains of α_{IIb}(989–1008) and α_V(987–1006). B) Sequence alignment of α_{IIb}(989–1008) and α_V(987–1006) with their structural regions highlighted. The structural regions of α_{IIb}(989-1008) were taken from PDB# 1DPK. C) Nomenclature and partial listing of the α_{IIb} and α_V cell-permeable peptides used in this study. The cell-permeable peptides used were N-terminal myristoylated. Exception: sIIb-2, sV-2 and their scrambled peptides (scr sIIb-2 and scr sV-2) – α β_3 signal peptide was inserted onto their N-terminus. The sequence in scr sIIb-2 and scr sV-2 prior to the hyphen is that of the β_3 signal peptide used. In the V-3 D-isomeric mutant peptide, V-3(d995-d998), the D-amino acids are displayed with lower case letters.

talin with m-calpain (Sigma). Human Fg was purified and labeled as previously described (42).

Peptide synthesis, purification, resuspension and characterization

Peptides were synthesized, cleaved and purified by reverse phase-HPLC on Vydac columns to a purity of ∃ **98%** and their molecular weights were confirmed by mass spectroscopy as previously described (23, 44). The N-terminal coupling of myristate and bromoacetate was performed following a standardized protocol (24). Facile formation of disulfide bonds in disulfide-cyclized peptides was carried out using Ekathiox resin (Sigma, Danvers, MA, USA). Fluorescent peptides were labeled on resin. A scrambled β_3(716–762) peptide with a N-terminal cysteine was kindly donated by Dr. G.C. White II (UNC, Chapel Hill, NC, USA). The peptides were dissolved in either aqueous buffers or buffers containing 10% ethanol. The maximum final concentration of ethanol that the cells were exposed to was 0.08%.

Circular dichroism spectroscopy and secondary structural analysis was performed as previously described (21).

Peptide internalization

The percentage of cell-bound peptides that were internalized by platelets and cells was determined by fluorescence quenching of FITC- and Oregon Green 488-labeled peptides(45). Fluorescence quenching was performed either by the addition of 0.2% Trypan blue (final concentration), or by centrifugation of the cell suspensions and then incubating the cells with anti-FITC antibodies for 30 minutes at 4°C. Fluorescence was measured on an EPICS Elite flow cytometer (Beckman Coulter, Fullerton, CA, USA) and a SpectraMax M2e microplate reader.

Surface plasmon resonance spectroscopy

Surface plasmon resonance (SPR) spectroscopy experiments were carried out on a Biacore-X (Biacore Inc. Piscataway, NJ, USA) located at the Saskatchewan Structural Sciences Centre. Peptides were coupled to carboxymethylated CM5 chips via N-terminal cysteines (22). Data was corrected for nonspecific binding using a sensor chip on which only cysteine was coupled. Surface plasmon resonance experiments were performed at 25°C using a running buffer composed of 20 mM Hepes, 10 mM NaCl, 1 mM $CaCl_2$, 0.05% surfactant P20, pH 7.2.

Molecular modeling

Molecular modeling studies were carried out using InsightII (Accelrys Inc., San Diego, CA, USA) as previously described (21). Molecular models for the transmembrane and CT of α_V were constructed by alignment of the sequence of α_V(987-1004) with α_{IIb}(985–1008) and imposing the NMR average structure of α_{IIb} CT (PDB# 1DPK) onto α_V. The initial structure for

α_V(1005–1018) was assigned using secondary structural predictions and CD analysis.

Cell adhesion assay

Cell adhesion experiments were performed using $\alpha_V\beta_3$-expressing cells and ligand-coated surfaces as previously described (17, 19). Briefly, Falcon 96-well microtitre plates were coated overnight at 4°C with 4 µg/well of Fg, prothrombin, vitronectin or BSA. The wells were rinsed and blocked for two hours with 1% BSA. Calcein AM-labeled cells (1 x 10^6 cells/ml.) were pretreated for 60 minutes at 37°C with peptides and then transferred to the ligand-coated plates for a one hour incubation in the presence or absence of 200 ng/ml PMA. The plates were washed three times with PBS and then counted on the SpectraMax M2e microplate reader.

Soluble ligand binding to platelets and cells

Fg binding to activated platelets was performed using gel-filtered platelets suspended in Tyrodes buffer (24). Briefly, platelets (3 x 10^8/ml) were preincubated for 30 minutes at 22°C with 300 nM ^{125}I-Fg and various concentrations of peptides. ADP (10 µM) and epinephrine (20 µM) were added and after a 30 minute incubation, 50 µl of each sample were loaded over a 20% sucrose solution and the tubes centrifuged. The tips of each tube were cut off and counted in a gamma counter. The binding of FITC-PAC1 and Oregon green488-Fg to gel-filtered platelets and cells were performed using a modified version of the Fg binding assay and by FACS analysis (16). The binding of ligands to activated platelets was performed in Tyrodes buffer containing 1 mM CaCl2, 1mM MgCl2, and 0.1% BSA and was monitored in the FL1 channel on the gated population of platelets from histograms.

Results

Effects of cell-permeable α peptides on β_3 integrin function

NMR structures of α_{IIb} CT revealed that the tail consists of a N-terminus helix, α_{IIb}(989–995), a central turn motif, α_{IIb}(995–1001), and a flexible acidic carboxyl-terminus α_{IIb}(1001–1008). Thus, overlapping α_{IIb} peptides (IIb peptide series) were synthesized to encompass all three of these structural regions (Fig. 1B and C). As the CT of α_V contains a homologous region to α_{IIb}, α_V(987–1006), a similar series of peptides were generated (V series). To endow cell-permeability to the peptides, either a N-terminal myristate or signal peptide was added. To confirm that the peptides were being internalized, a number of them were fluorescently labeled and their % internalization were calculated by fluorescence quenching (Fig. 2). As expected, proteins, non-cell-permeable peptides (soluble V-1) or large peptides (β_3 CT) were not efficiently internalized, while all other peptides of equivalent sequence length were equally internalized to a maximum of 50% (Fig. 2B). Thus, any difference in the functional capacity of an α_{IIb} peptide versus its α_V counterpart was not due to differences in their % internalization. In addition, none of the control or myristoylated peptides tested exhibited any toxic side effects as evaluated using the MTT assay (data not shown).

V-1 and IIb-1 were first used to begin the comparison between α_V and α_{IIb} peptides. Pretreatment of platelets with increasing amounts of IIb-1, resulted in a dose-dependant decrease in agonist-induced Fg binding to $\alpha_{IIb}\beta_3$ (Fig. 3A), while V-1 had no effect. Similar results were also obtained by flow cytometry using TRAP as the stimulus (Fig. 3B). Trap stimulation resulted in a 140-fold increase in Fg binding which was inhibited equally by cRGD peptide and IIb-1, while V-1 was ineffective. To test the effect of the CT peptides on $\alpha_V\beta_3$ activation, cell adhesion experiments were performed. In this $\alpha_V\beta_3$ functional assay, pretreatment of GM1500s with IIb-1 had no effect on PMA-induced cell adhesion, while V-1 completely blocked the stimulated cell

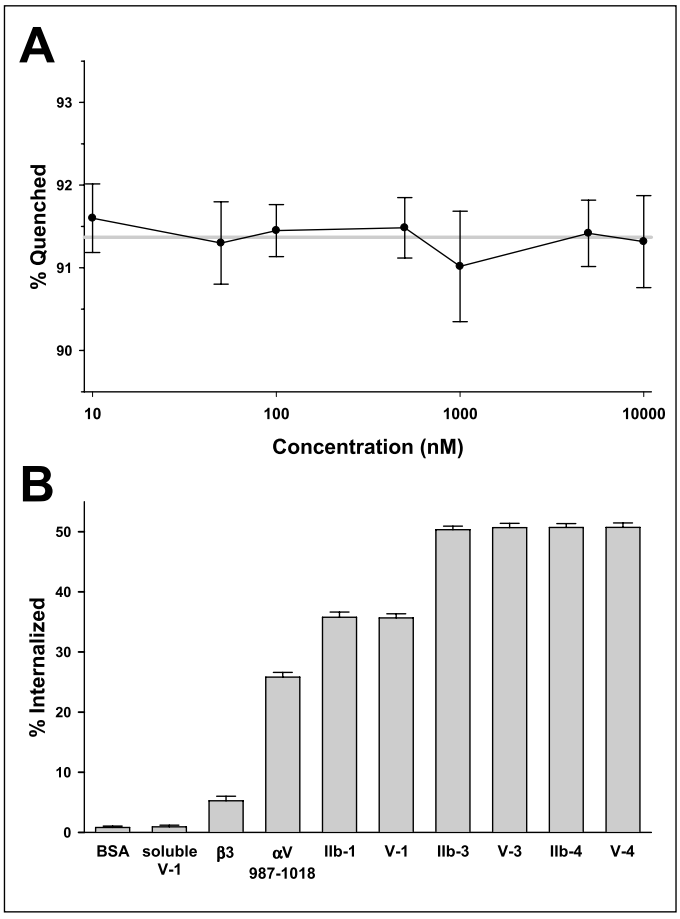

Figure 2: Cell-permeable peptide internalization. A) Linearity of fluorescence quenching. The capacity of 0.2% trypan blue to quench the fluorescence of solvent exposed Oregon Green 488-labeled V-3 is linear over a wide concentration range. Varying amounts of Oregon Green 488-labeled V-3 were placed in 96 well plates and after a five minute incubation with 0.2% trypan blue, fluorescence was measured. Grey lines represent the mean of all concentrations. Similar results were obtained using other fluorescent-labeled peptides and proteins. B) Effect of myristoylation and peptide size on internalization. Platelets were preincubated with fluorescent-labeled proteins and peptides for one hour, treated with ± 0.2% trypan blue for five minutes and then their fluorescence was measured. The fluorescence units were converted into % internalization using mean maximal quenching value of 91.4% for a solvent exposed fluorochrome, as determined in panel A. All peptides tested of similar sequence length were equally internalized, regardless of the charge on the peptide. Similar results were obtained when the fluorescence was quantitated by flow cytometry, with GM1500 cells, or when the platelets were washed and the fluorescence was quenched using anti-fluorescein antibodies.

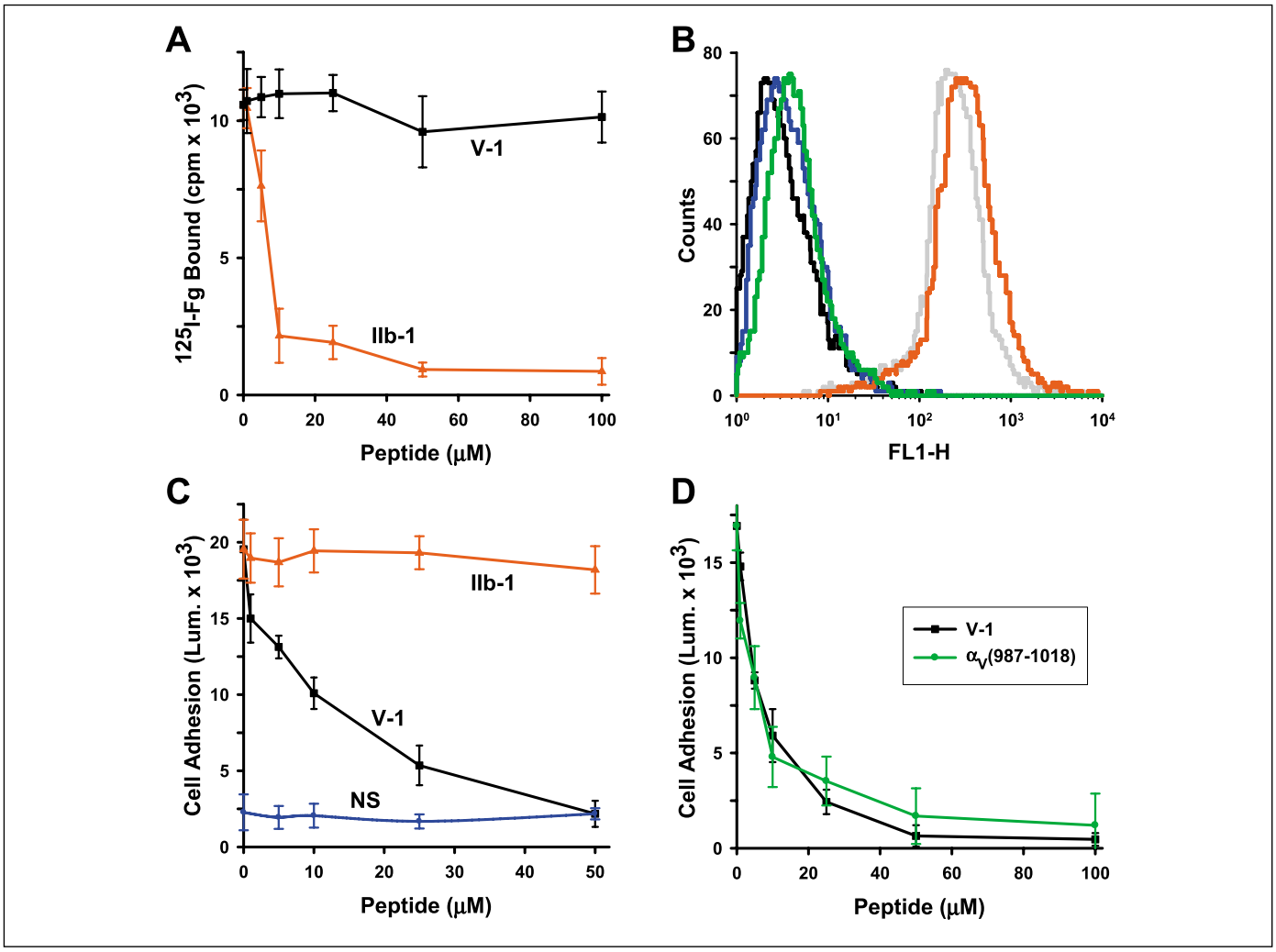

Figure 3: Specificity in the inhibition of $\alpha_V\beta_3$ and $\alpha_{IIb}\beta_3$ activation by α CT peptides. A) IIb-1 suppressed $\alpha_{IIb}\beta_3$ activation. Washed platelets were preincubated for 30 minutes with 300 nM ^{125}I-Fg and varying concentrations of IIb-1 or V-1. Fg binding was then measured 30 minutes following the addition of ADP and epinephrine. Peptide pretreatment had no effect on basal Fg binding to non-stimulated platelets. The data are expressed as mean ± S.D. performed in quintuplicate and are representative of three separate experiments. B) Fg binding as assessed by flow cytometry. Platelets were pretreated with peptides as described in panel A using Oregon Green 488-labeled Fg. Platelets were stimulated with 10 μM TRAP and Fg binding was measured by flow cytometry. Nonstimulated platelets, black line; ADP/epinephrine stimulated, red line; IIb-1, green line; V-1, grey line; 250 μM cRGD peptide, blue line. Similar results were obtained using FITC-PAC1 as the ligand or ADP/epinephrine as the stimulus. The data are representative of three separate experiments, each performed in triplicate. C) V-1 suppression of $\alpha_V\beta_3$ activation. GM1500s were pretreated with peptides and following the addition of 200 ng/ml PMA, cell adhesion to vitronectin-coated plates was measured. IIb-1, red line; V-1, black line; non-stimulated cells (NS) incubated with V-1, blue line. The data are expressed as mean ± S.D. performed in quintuplicate and are representative of three separate experiments. (D) V-1 and α_V(987–1018) suppression of $\alpha_V\beta_3$ activation. Experiments were performed as described in panel C using prothrombin-coated wells. Pretreatment with V-1 or α_V(987–1018) blocked stimulated GM1500 cell adhesion. Non-stimulated Fg binding and cell adhesion levels were subtracted from values in panels A and D (0.357 x 10^3 cpm and 2.508 x 10^3 units, respectively).

adhesion (Fig. 3C). Thus, completely opposite results were obtained with the two peptides depending on which integrin family member mediates the biological process being assayed. Similarly, V-1 was inhibitory when vitronectin was replaced with prothrombin as the $\alpha_V\beta_3$-ligand, and α_V(987–1018), which encompasses the entire CT of α_V, also inhibited $\alpha_V\beta_3$ activation (Fig. 3D). The stimulated cell adhesion was determined to be $\alpha_V\beta_3$-specific as treatment with $\alpha_V\beta_3$ function-blocking antibodies LM609 and 7E3, resulted in ≥ 95% inhibition of the PMA-stimulated adhesion. The specificity and the intracellular mode-of-action was also confirmed as non-myristoylated peptides, myristoylated non-CT peptides, and myristic acid were all devoid of activity.

Determining the biological activity of cell-permeable peptides derived from the α CTs of β_3 integrins

As both IIb-1 and V-1 contained biological activity, the next set of experiments was performed to determine whether their biological activity could be restricted to a structural region. Previously, it had been demonstrated in studies that

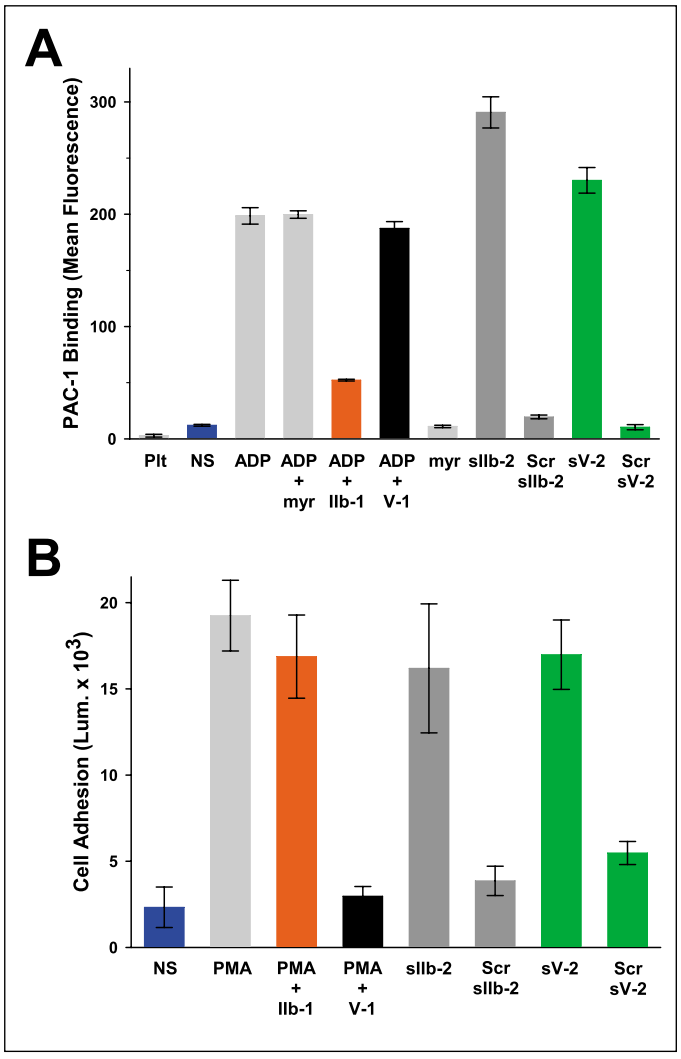

Figure 4: Effect of N-terminal α CT peptides on integrin activation. A) N-terminal α CT peptides derived from both α_{IIb} and α_V activate $\alpha_{IIb}\beta_3$ independent of a cell agonist. Platelets were incubated with 20 μg/ml FITC-labeled PAC-1 alone (ADP) or with 50 μM of myristic acid (ADP + myr), IIb-1 (ADP + IIb-1) or V-1 (ADP + V-1). Thirty minutes after the addition of the stimulus, PAC-1 binding was measured by flow cytometry. ADP and epinephrine (ADP) resulted in a 72-fold increase in PAC-1 binding in comparison to non-stimulated platelets (NS). Control non-stimulated platelets in the absence of PAC-1 (Plt) are displayed. To measure the capacity of IIb-2 and V-2 to activate platelets, platelets incubated with PAC-1 were treated with 1 mM of myristic acid (myr), sIIb-2, sV-2, or scrambled peptides (Scr sIIb-2 and Scr sV-2), and 30 minutes later PAC-1 binding was measured. No additive effect on PAC1 binding was observed when ADP and epinephrine were added to platelets treated with sIIb-2. Data are expressed as geometric mean fluorescence ± S.D., performed in quadruplicate and are representative of two separate experiments. B) N-terminal CT peptides derived from α_{IIb} or α_V activate $\alpha_V\beta_3$. GM1500 PMA-stimulated cell adhesion to prothrombin-coated plates were measured following pretreatment with either buffer (PMA), or with 50 μM of IIb-1 (PMA + IIb-1) or V-1 (PMA + V-1). V-1, but not IIb-1, blocked the stimulated adhesion to non-stimulated (NS) levels. Cell adhesion was also measured in the absence of PMA following the addition of one mM of sIIb-2, Scr sIIb-2, sV-2, or Scr sV-2. Thus, both sIIb-2 and sV-2 can activate $\alpha_V\beta_3$. Similar results were obtained using vitronectin-coated plates. Experiments were performed in quadruplicate and are representative of three separate experiments.

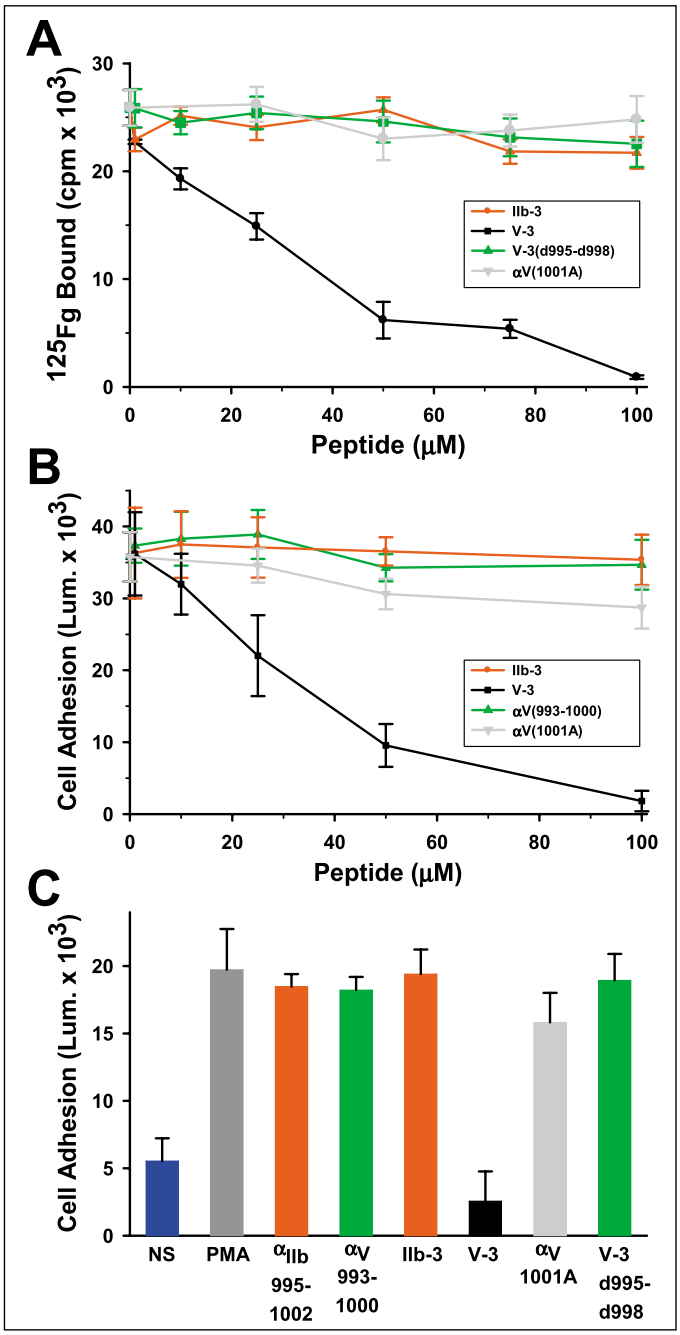

Figure 5: A functionally active α_V turn-motif peptide. A) The central turn peptide of α_V suppresses Fg binding to platelets. The effect of IIb-3, V-3, an optical isomeric V-3 peptide [V-3(d995-d998)], or α_V(1001A) on stimulated Fg binding to platelets were measured as described in Figure 3A. Of the four peptides tested, only V-3 was inhibitory. B) The central turn peptide of α_V suppresses $\alpha_V\beta_3$-mediated cell adhesion. PMA-stimulated cell adhesion to vitronectin was performed as described in Figure 3C. GM1500s were pretreated with increasing concentrations of IIb-3, V-3, α_V(993–1000) or α_V(1001A). Only V-3 was inhibitory. C) α_V(Q1001) is a biologically critical residue. Stimulated GM1500 cell adhesion to vitronectin was performed as described in Figure 3C. Only pretreatment with 100 μM of V-3 blocked the PMA-stimulated adhesion. α_{IIb}(995–1002), α_V(993–1000), IIb-3, α_V(1001A), and V-3(d995-d998), and control cell-permeable peptides containing a turn motif, RANITYRG and RANPLYRG, were all non-inhibitory. None of the peptides used in these experiments altered non-stimulated Fg binding or cell adhesion levels (data not shown).

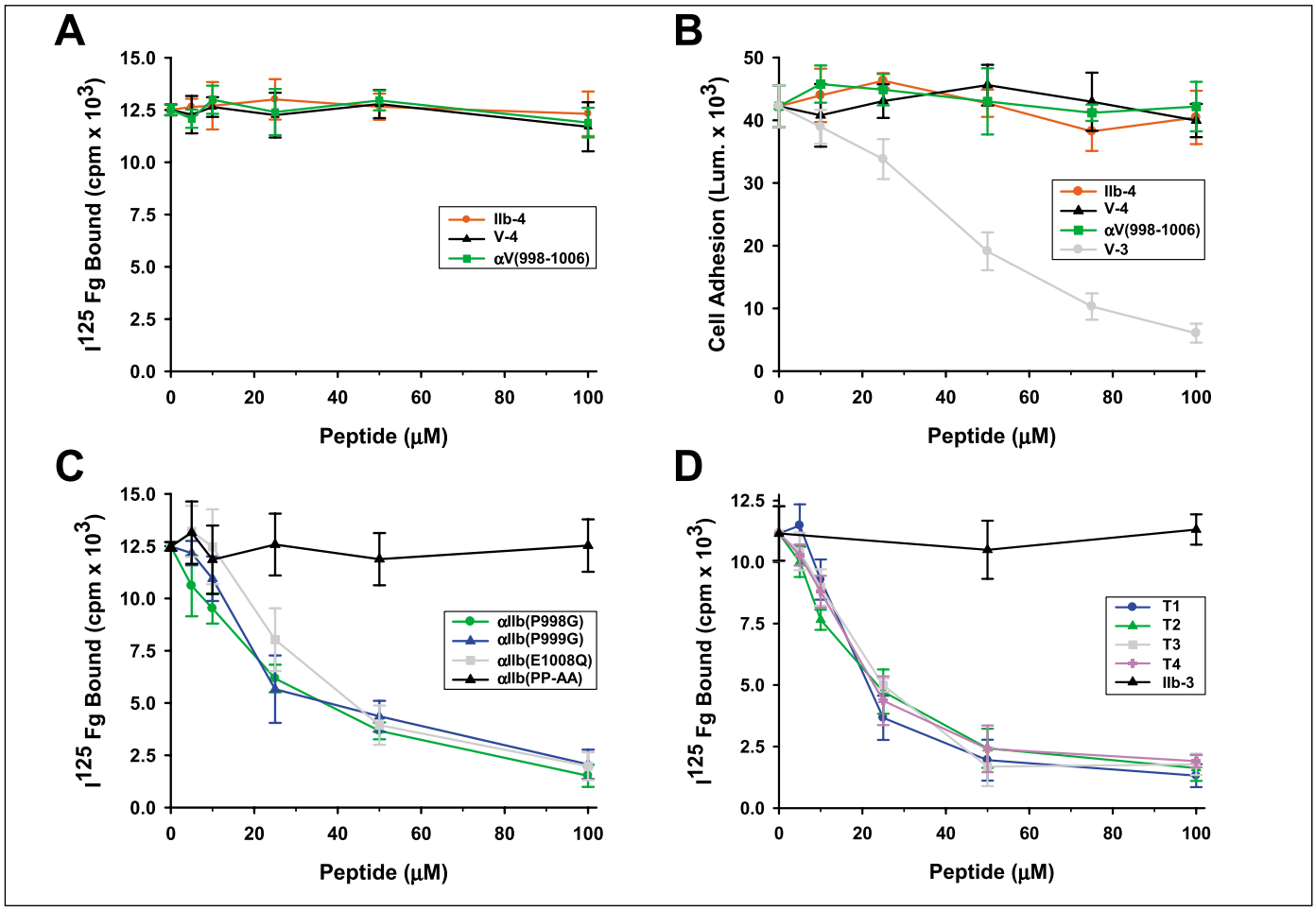

Figure 6: Assessing the capacity of C-terminal and α_{IIb} turn-motif peptides to suppress β_3 integrin activation. A) The C-terminal α CT peptides do not influence Fg binding to platelets. The effects of pretreatment with IIb-4, V-4, or an extended V-4 peptide [α_V(998–1006)] on Fg binding to stimulated platelets were evaluated as described in Figure 3A. None of the peptides were inhibitory while pretreatment with 100 μM IIb-1 decreased Fg binding to nearly non-stimulated levels (1394 ± 206 cpms). B) C-terminal peptides do not influence $\alpha_V\beta_3$-mediated cell adhesion. PMA-stimulated GM1500 cell adhesion to vitronectin was not blocked by pretreatment with IIb-4, V-4, or α_V(998–1006), while V-3 was inhibitory. Experiments were performed as described in Figure 3C. C) Effect of mutated α_{IIb} CT peptides on Fg binding to stimulated platelets. The effects of pretreatment with α_{IIb}(PP-AA), α_{IIb}(E1008Q), α_{IIb}(P998G) and α_{IIb}(P999G) on Fg binding to stimulated platelets were evaluated as described in Figure 3A. All peptides were as effective as IIb-1 (1394 ± 206 cpms, at 100 μM) in reducing Fg binding, with the exception of α_{IIb}(PP-AA). D) Effect of truncated α_{IIb} CT peptides on Fg binding to stimulated platelets. Experiments were performed as described in panel C using IIb-3, and truncation peptides T1, T2, T3, and T4. Only IIb-3 was non-inhibitory.

α_{IIb}(K989-R995) can activate $\alpha_{IIb}\beta_3$ (38, 39). Therefore, myristoylated forms of this peptide and its homologous α_V sequence were synthesized (IIb-2 and V-2, Fig. 1) and tested for biological activity. However, considerable data variation occurred using these peptides; therefore IIb-2 and V-2 were resynthesized with a β_3 signal peptide added to endow cell-permeability (sIIb-2 and sV-2, respectively). The addition of 1 μM of sIIb-2 or sV-2 induced PAC-1 binding, even greater than that induced by ADP/epinephrine stimulation (Fig. 4A). Myristic acid and scrambled peptides were functionally silent. sIIb-2 and sV-2 also induced Fg binding to platelets and the formation of platelet aggregates (data not shown). When added to GM1500s, sIIb-2 and sV-2 caused a marked increase in cell adhesion, equal to levels obtained using PMA (Fig. 4B). Thus, the N-terminus of the CT of both α_V and α_{IIb} are capable of activating β_3 integrins.

IIb-3 and V-3 were the next set of peptides to be examined. Preincubation of platelets and BAECs with V-3 inhibited ADP/EPI induced Fg binding and PMA-induced cell adhesion (Fig. 5A and 5B), while IIb-3 was inactive. To confirm that IIb-3 was biologically silent, two cyclized versions of IIb-3 were synthesized using disulfide and thioether linkages. Both cyclic IIb-3 peptides were inactive while the two corresponding cyclic V-3 peptides had similar potency as V-3. C-terminal truncation peptides of V-3 and IIb-3, α_V(993–1000) and α_{IIb}(995–1002), were both inactive (Fig. 5B and 5C). These data indicated that α_V(Q1001) was required for endowing biological activity to V-3, as its truncation from α_V(993–1001) resulted in an inactive peptide. To verify if the side chain atoms of α_V(Q1001) were essential for endowing biological activity to V-3, an α_V(Q1001) to alanine mutant peptide was tested, α_V(1001A). This peptide ex-

hibited little to no activity (Fig. 5A, 5B and 5C). Thus, the side chain atoms of α_V(Q1001) endowed biological activity to V-3. As the major structural feature within V-3 is a turn, a mutant V-3 peptide was synthesized with D-amino acids incorporated into positions occupied by the turn, V-3(d995-d998). When tested, V-3(d995-d998) was also inactive (Fig. 5A, 5C).

Finally, the capacity of the C-terminal α_V and α_{IIb} peptides to block β_3 integrin-mediated Fg binding and cell adhesion were evaluated. Both C-terminal peptide (IIb-4 and V-4) had no effect on Fg binding (Fig. 6A). Equally inactive was α_V(998–1006), a N-terminal extension of V-4. All three peptides were also ineffective at altering PMA-stimulated cell adhesion (Fig. 6B). Thus, the C-terminal region of α_{IIb} and its homologous counterpart in α_V were functionally inactive.

The foregoing experiments revealed that only the sequence in V-1 responsible for inhibiting $\alpha_V\beta_3$-mediated cell adhesion was minimized to V-3, while the inhibitory sequence of IIb-1 was still unaccounted for. Therefore, a series of mutant and truncated α_{IIb} peptides were constructed and their capacity to block Fg binding to activated platelets was evaluated (Fig. 6C and 6D). As a control, the double proline mutant peptide of IIb-1, α_{IIb}(PP-AA), was shown to be non-inhibitory (Fig. 6C). As this mutation resulted in misfolding of α_{IIb} (24), more structurally conservative single glycine mutant peptides were synthesized [α_{IIb}(P998G) and α_{IIb}(P999G)]. Conservation of the secondary structural composition of α_{IIb} CT was confirmed by CD. In contrast to α_{IIb}(PP-AA), at 100 μM both α_{IIb}(P998G) and α_{IIb}(P999G) were as effective as IIb-1 at blocking Fg binding (Fig. 6C). Thus, the side chains of the prolines in the turn of α_{IIb} CT were not essen-

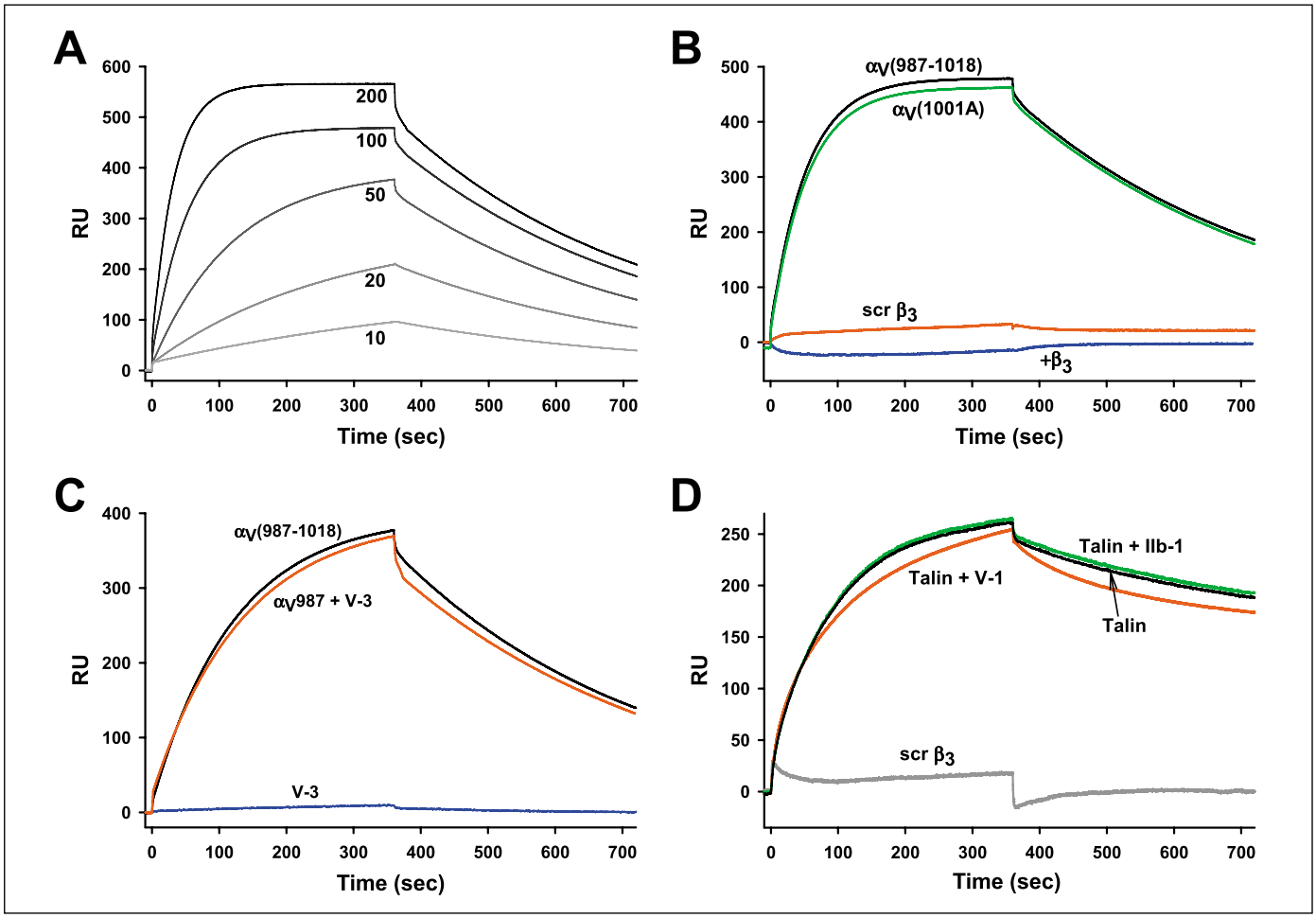

Figure 7: Surface plasmon resonance analysis of the effect of CT peptides on cytosolic complexes. A) Formation of a cytoplasmic complex between α_V and β_3. β_3(716–762) with an N-terminal cysteine was coupled to a CM5 sensor chip via thiol linkage. Increasing concentrations (10 to 200 μM) of α_V(987–1018) were passed across the β_3-coated chip for 360 seconds, followed by a dissociation phase of an additional 360 seconds. Similar affinity constants were obtained using chips on which three and ten-fold less b_3(716–762) was coupled. B) Specificity of interaction. Specificity was confirmed by passing 100 μM α_V(987–1018) over β_3(716-762)-coated (black line) versus a scrambled β_3(716–762)-coated chip (scr b3), and by preincubating α_V(987–1018) for one hour with a five-fold excess of soluble β_3(716–762) (+b3) prior to injection. For comparison, 100 μM α_V(1001A) was also passed over the β_3(716–762)-coated chip (green line, offset by –10 RU). C) V-3 did not block α_V/β_3 cytoplasmic complex formation. Fifty μM α_V(987–1018), 200 μM V-3, or 50 μM α_V(987–1018) plus 200 μM V-3 were passed over the β_3(716–762)-coated chip. D) Influence of CT peptides on Talin-H binding to β_3. 100 nM of talin-H was passed over CM5 sensor chips coated with either β_3(716–762) (black line) or a scrambled β_3(716–762) peptide (scr β3). Talin-H was also preincubated for one hour in solution with 200 μM IIb-1 (green line) or V-1 (red line) prior to injection.

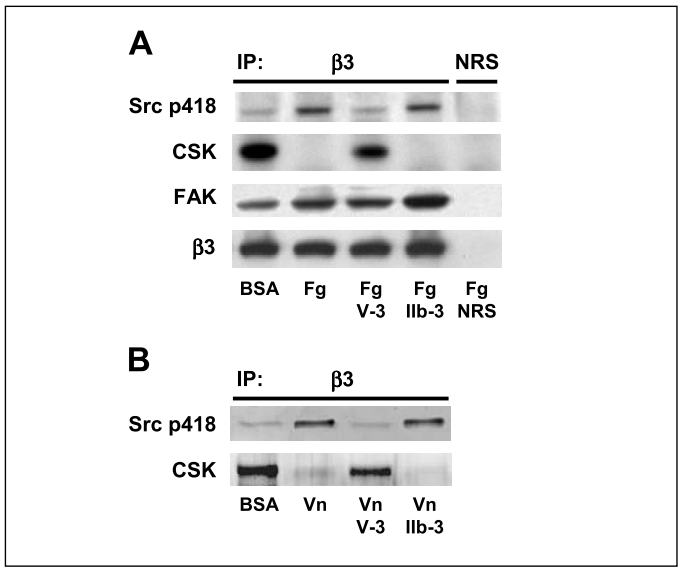

Figure 8: Blockage of Csk dissociation and Src phosphorylation by V-3. A) Blockage in platelets. Gel-purified platelets were suspended in HEPES-modified Tyrodes buffer and allowed to adhere to a Fg matrix for one hour or allowed to remain in solution over a BSA matrix (BSA). Platelets were preincubated for 30 minutes with either buffer alone (BSA, Fg and Fg NRS) or with 100 μM of V-3 (Fg V-3) or IIb-3 (Fg IIb-3) prior to plating over Fg-coated wells. The platelets were lysed with detergent and the soluble fraction was immunoprecipitated with a polyclonal antibody to β_3 (β_3, first four lanes) or with a normal rabbit serum (last lane). Immunoprecipitates were probed on Western blots with antibodies to p418-Src, Csk, FAK, and β_3. Data shown are representative of three separate experiments. B) Blockage in GM1500 cells. Experiments in panel A were repeated using GM1500 cells adhering to vitronectin (Vn) and probing the blots with anti-p418-Src and anti-Csk antibodies.

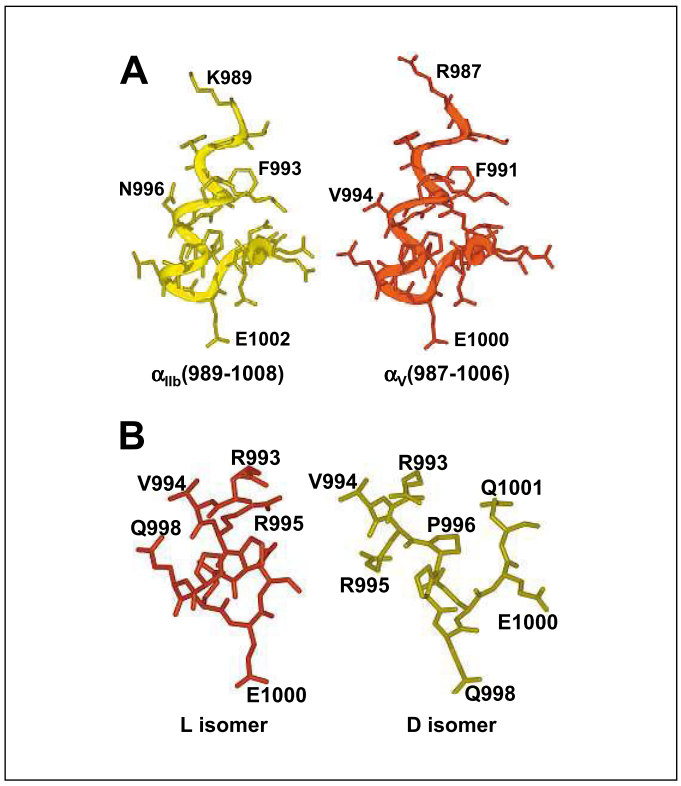

Figure 9: Structural models of the α CTs of β_3 integrins. A) Structure of α_{IIb}(989–1008) and α_V(987–1006). Molecular models of the α_V CT were generated using the NMR backbone structure of α_{IIb}(989-1008) (yellow left structure) as a starting template. Displayed is the initial α_V substituted structure of α_V(987-1006) (red right structure) which shows that the position of N996 and L1000 in α_{IIb} are swapped in α_V (Q998 and V994). B) D isomeric replacement of the α_V(995-998) resulted in major backbone and side chain realignments. The L-amino acids in α_V(995–998) were replaced with D-residues and the resulting structure was allowed to relax into a minimized structure. The original L structure (red) and the D structure (yellow) are displayed in stick fashion using the backbone structure of α_V(989–994) to align the two structures. The conformational changes that occurred to allow for the reorientation of the side chains resulted in spatial replacement of several amino acids, such as Q998 replaced with R995, and E1000 with Q998. Heavy atoms are only displayed in both panels and the position of a number of side chains are indicated.

tial for endowing inhibitor capacity to IIb-1. Similarly, the C-terminal glutamate was not required for inhibitor capacity, as α_{IIb}(E1008Q) was inhibitory. This result was further confirmed using a series of C- and N-terminal truncation peptides, T1-T4 (Fig. 1C). All four truncation peptides were inhibitory, while IIb-3 was not (Fig. 6D). Thus, T4 was the shortest a_{IIb} peptide tested that still retained inhibitory capacity.

Capacity of α CT peptides to form and to disrupt intracellular complexes

Experiments were performed to determine whether the capacity of the CT peptides to block integrin activation was a result of them interfering with the interaction of the cytoplasmic tails with an intracellular binding partner. The three binding partnerships that were assessed were: the α-β integrin CT complex (23), the talin-β_3 complex (28, 46), and the association of kinases with the β_3 CT (27).

While studies have demonstrated that the CTs of $\alpha_{IIb}\beta_3$ interact to form a complex (22, 23), none have established that this is a general property of integrins, and whether the CTs of $\alpha_V\beta_3$ interact with each other. Therefore, the interaction of α_V and b_3 CTs was examined and characterized by SPR (Fig. 7). The interaction of α_V(987–1018) with β_3(716–762) was assessed by passing increasing amounts of α_V(987–1018) across a β_3(716–762)-coated chip (Fig. 7A). Combined analysis of the association and dissociation phases generated a dissociation constant K_d of 23.6 ∀ 4.9 μM. Formation of the α_V and β_3 complex was specific as replacement of β_3(716–762) on the chip with a scrambled peptide or preincubation of the α_V(987–1018) buffer with a five-fold excess of soluble β_3(716–762) abolished complex formation (Fig. 7B). In contrast to α_V(987-1018), V-3 failed to interact with β_3(716–762) (Fig. 7C). Furthermore, the addition of 200 μM of V-3 during the association and dissociation phases of α_V(987–1018) with β_3(716–762) had minimal impact. Thus, it appeared unlikely that the capacity of V-3 to block β_3 integrin activation was related to a direct perturbation of the α/β CT complex.

Since a number of studies have proven that talin-H is a possible activator of $\alpha_{IIb}\beta_3$ (28, 43), experiments were performed to see if the inhibitory capacity of IIb-1 or V-1 was related to the capacity of these peptides to interfere with the binding of talin-H to

β_3(716–762). Passage of a running buffer containing 100 nM talin-H over a β_3(716–762)-coated sensor chip resulted in high affinity interaction of talin-H with β_3 (K_d = 3 nM). The addition of 200 μM of IIb-1 or V-1 to the running buffer during the association and dissociation phases did not alter this interaction (Fig. 7D). Therefore, the inhibitory capacity of IIb-1 or V-1 did not involve talin-H binding.

The third interaction that was assessed was between the association of kinases with the β_3 CT (Fig. 8). Human platelets were incubated over a non-adherent BSA matrix or a Fg matrix to which they adhere and spread on. The platelets were solubilized and immunoprecipitation of $\alpha_{IIb}\beta_3$ from platelets demonstrated that FAK and Csk were associated with ligand-free $\alpha_{IIb}\beta_3$ (BSA), but that Csk dissociated from $\alpha_{IIb}\beta_3$ when it was bound to Fg. The decrease in Csk was associated with an increase in tyrosine-418 phosphorylated Src (Src-p418), a marker of Src activation. Pretreatment of the platelets with 100 mM of V-3 resulted in a blockage of Src phosphorylation and retention of Csk. Similar results were obtained using GM1500 cells. In contrast, IIb-3 pretreatment had no effect. FAK levels remained unaltered by all treatment conditions. Thus, the inhibitory activity of V-3 towards integrin activation may be a result of V-3 disrupting the coordination in the binding of Csk and possibly other kinases, but not FAK, with the β_3 CT.

Discussion

Previous studies have indicated that interaction between the integrin $\alpha_{IIb}\beta_3$ two cytoplasmic domains regulates its activation, and that the CT of α_{IIb} plays a major role in this regulation. In the present work, it was demonstrated that the CT of α_V also regulates integrin activation and sequences within both α CTs that mediated this regulation were identified. Of most interest were three novel findings: 1) cell-permeable α_V cytoplasmic peptides can block β_3 integrin activation in a subfamily-specific manner; 2) α_VQ1001 in the CT of α_V was identified as a critical residue in suppression of $\alpha_V\beta_3$ activation; and, 3) the inhibitory capacity of the α CT peptides was associated with their capacity to disrupt the interaction of the integrin CT with Csk and Src activation.

In regards to the use of CT peptides for the development of anti-cancer and anti-platelet therapeutics, α_V(987–1006) blocked $\alpha_V\beta_3$-mediated cell adhesion while α_{IIb}(989–1008) was completely ineffective (Fig. 3), and conversely α_{IIb}(989-1008) blocked Fg binding to platelets while α_V(987–1006) was silent. These two homologous sequences differ in identity at nine sites, including two substitutions proximal to the PP-turn motif. Comparison of the NMR structure of α_{IIb} versus molecular models of α_V (Fig. 9A) revealed that the reversal in position of the two amino acids proximal to the turn motif resulted in the swapping of a hydrophobic residue with a hydrophilic hydrogen-bonding residue. If these two residues are important for intracellular ligand binding, this swapping may, in part, account for the functional specificity of the two peptides.

The unique C-terminal extension of α_v, α_V(1007–1018), does not appear to play a major role in regulating integrin activation as the capacity of α_V(987–1018) to suppress $\alpha_V\beta_3$ activation was similar to that of α_V(987–1006) (Fig. 3). The acidic C-terminus of α_{IIb} and its homologous sequence in α_v, peptides IIb-4 and V-4, were both functionally silent (Fig. 6). In α_v, the minimal CT sequence with inhibitory capacity was defined by α_V(993–1001), while its α_{IIb} counterpart [α_{IIb}(995–1003), IIb-3] was inactive (Fig. 5). Others have reported that IIb-3 has activity (41). However, herein IIb-3 and cyclized versions of this peptide were all biologically inactive. These differences in the activity of IIb-3 may be a result of differences in the design of the cell-permeable peptides – palmitoylated versus myristoylated and/or amide versus carboxyl terminus. However, extension of IIb-3 by four amino acids resulted in an active peptide (T4, α_{IIb}(993-1005); Fig. 6D). Therefore, this and the previous study both determined that α_{IIb}(993–1005) contains the inhibitory domain of the α_{IIb} CT. As to the mode-of-action of the minimalized peptide, the capacity of the CT peptides to suppress integrin activation was not related to a perturbation of the α/β CT complex, as α_V(993–1001) had low affinity for β_3 and was ineffective at preventing the a_V CT from interacting with β_3 (Fig. 7).

Previous studies demonstrated that α_{IIb}(989–997) can activate $\alpha_{IIb}\beta_3$ in a cell-agonist independent manner (38, 39). Using a signal peptide attached to the N-terminus of α_V(987–995) as the means of endowing cell-permeability, α_V(987–995) was shown to contain similar integrin activation properties (Fig. 4). Studies have shown that CIB1 interacts with α_{IIb}(983–997), which encompasses α_{IIb}(989–997), but it does not interact with the CT of α_V (22, 33, 40). Recently, it was demonstrated that CIB1 can inhibit agonist-induced $\alpha_{IIb}\beta_3$ activation by disruption of talin binding to the β_3 CT (37). Thus, while the activation of integrins by α_{IIb}(989–997) may in part be attributed to CIB1, it is unlikely that the capacity of α_V(987–995) to activate integrins involved CIB1. The head domain of talin (talin-H) is a putative activator of $\alpha_{IIb}\beta_3$ (28, 43). Using platelet-derived talin-H, high affinity binding of talin-H to β_3 was confirmed (Fig. 7). In contrast to CIB1 (37), neither α_{IIb}(989–1008) nor α_V(987–1006) blocked talin-H binding to β_3. Thus, the inhibitory capacity of these peptides was not related to a disruption in talin-H binding. Other studies have identified kinases that interact or become associated with the cytoplasmic domain of integrins. Some of these kinases are possible candidate proteins whose interaction with integrin CTs is perturbed by the synthetic a cytoplasmic peptides. Of these kinases, Csk, Syk and Src are likely candidates (27, 47).

In this study, V-3 and IIb-3, α_V(993-1001) and α_{IIb}(995–1003), respectively, were tested for their capacity to influence the binding of kinases to $\alpha_{IIb}\beta_3$. α_V(993–1001) but not α_{IIb}(995–1003) inhibited the dissociation of Csk from the β_3 CT and subsequent activation of Src. Thus the inhibitory capacity of α_V(993-1001) to block integrin activation may be due to its capacity to disrupt the intracellular mechanisms involved in coordination the binding of Csk with the β_3 CT. More detailed experiments are required to identify the complex mechanism(s) involved in regulating the association and dissociation of Csk from the β_3 CT, and subsequently how α_V(993–1001) interferes with this regulation.

Our previous study indicated that a major structural feature in the CT of α_{IIb} was its turn motif and that destruction of this turn resulted in a biologically inactive peptide (24). Given the high sequence homology between α_{IIb}(989-1008) and α_V(987-1006) and the functional data presented herein, a number of control peptides were used to determine what features

of the turn are required for this biological activity. Single glycine substitutions of α_{IIb}(989–1008) at α_{IIb}(P998) and α_{IIb}(P999) remained inhibitory while the double proline mutant α_{IIb} peptide, α_{IIb}(PP-AA), was inactive (Fig. 6C). Similar to α_{IIb}(PP-AA), replacement of the amino acids that form the turn in α_V CT with their optical D isomers (D-amino acids) abolished the capacity of α_V(993–1001) to block integrin activation (Fig. 5A). Structurally, the double proline to alanine mutation resulted in a misfolded tail (PDB# 1PDQ) while the more conservative single glycine mutant peptides preserved the structural composition of α_{IIb} CT. The L- to D-amino acid conversion resulted in the preservation of the turn structure (Fig. 9B), but the direction of the fold and the spatial orientation of the side chains were reversed. Therefore, it was concluded from these findings that the side chain atoms of the prolines present in the turn of these two α CTs most likely do not directly participate in endowing the inhibitor capacity to the CT peptides. However, the backbone structure of the turn formed by these prolines.

Finally, the truncation peptide α_V(993–1000) was biologically silent, while α_V(993–1001) was potent at suppressing β_3 integrin activation. Mutation of glutamine 1001 into alanine, α_V(Q1001), resulted in a peptide that exhibited minimal functional activity. Thus, the side chain atoms of α_V(Q1001) endowed biological activity to α_V CT peptides. However, the minimalized α_V CT peptide, V-3, did lose the specificity exhibited by its parent peptide in suppressing only $\alpha_V\beta_3$ activation. Identifying the residues responsible for the integrin family member specificity of both α_V and α_{IIb} peptides will allow for the development of anti-cancer/anti-angiogenesis versus anti-platelet therapeutics.

Acknowledgements

The author thanks Dr. Gilbert C. White for reagents, Tangyne Berry for technical assistance, and Dr. Vanina DalBello-Haas for her technical advice and critical review of the manuscript.

References

1. Hynes RO. Integrins: versatility, modulation, and signaling in cell adhesion. Cell 1992; 69: 11–25.
2. Ruoslahti E. Integrins. J Clin Invest 1991; 87: 1–5.
3. Hughes PE, Pfaff M. Integrin affinity modulation. Trends Cell Biol 1998; 8: 359–364.
4. Chen Y-P, Djaffar I, Pidard D, et al. Ser-752 to Pro mutation in the cytoplasmic domain of integrin β_3 subunit and defective activation of platelet integrin $\alpha_{IIb}\beta_3$ (glycoprotein IIb-IIIa) in a variant of Granzmann thrombasthenia. Proc Natl Acad Sci USA 1992; 89: 10169–10173.
5. O'Toole TE, Katagiri Y, Faull RJ, et al. Integrin cytoplasmic domains mediate inside-out signal transduction. J Cell Biol 1994; 124: 1047–1059.
6. Xiong JP, Stehle T, Diefenbach B, et al. Crystal structure of the extracellular segment of integrin $\alpha_V\beta_3$. Science 2001; 294: 339–345.
7. Xiong JP, Stehle T, Zhang R, et al. Crystal structure of the extracellular segment of integrin a_V b3 in complex with an Arg-Gly-Asp ligand. Science 2002; 296: 151–155.
8. Xiao T, Takagi J, Coller BS, et al. Structural basis for allostery in integrins and binding to fibrinogen-mimetic therapeutics. Nature 2004; 432: 59–65.
9. Yamanouchi J, Hato T, Tamura T, et al. Identification of critical residues for ligand binding in the integrin β3 I-domain by site-directed mutagenesis. Thromb Haemost 2002; 87: 756–762.
10. Perkins KB, Loftus JC. A mutation in the integrin αIIb subunit that selectively inhibits aIIbb3 receptor function. Thromb Haemost 2003; 90: 853–862.
11. Tamura T, Hato T, Yamanouchi J, et al. Critical residues for ligand binding in blade 2 of the propeller domain of the integrin αIIb subunit. Thromb Haemost 2004; 91: 111–118.
12. Honda S, Kashiwagi H, Kiyoi T, et al. Amino acid mutagenesis within ligand-binding loops in alpha v confers loss-of-function or gain-of-function phenotype on integrin αvβ3. Thromb Haemost 2004; 92: 1092–1098.
13. Phillips DR, Nannizzi-Alaimo L, Prasad KS. β3 tyrosine phosphorylation in αIIbb3 (platelet membrane GP IIb-IIIa) outside-in integrin signaling. Thromb Haemost 2001; 86: 246–258.
14. Shattil SJ, Gao J, Kashiwagi H. Not just another pretty face: regulation of platelet function at the cytoplasmic face of integrin $\alpha_{IIb}\beta_3$. Thromb Haemost 1997; 78: 220–225.
15. Hughes PE, Diaz-Gonzalez F, Leong L, et al. Breaking the integrin hinge: a defined structural constraint regulates integrin signaling. J Biol Chem 1996; 271: 6571–6574.
16. Helluin O, Chan C, Vilaire G, et al. The activation state of αvβ3 regulates platelet and lymphocyte adhesion to intact and thrombin-cleaved osteopontin. J Biol Chem 2000; 275: 18337–18343.
17. Pampori N, Hato T, Stupack DG, et al. Mechanisms and consequences of affinity modulation of integrin a_Vb_3 detected with a novel patch-engineered monovalent ligand. J Biol Chem 1999; 274: 21609–21616.
18. Hughes PE, O'Toole TE, Ylänne J, et al. The conserved membrane-proximal region of an integrin cytoplasmic domain specifies ligand binding affinity. J Biol Chem 1995; 270: 12411–12417.
19. Finberg RW, Cheresh DA. A β turn in the cytoplasmic tail of the integrin α_v subunit influences conformation and ligand binding of $\alpha_v\beta_3$. J Biol Chem 1994; 269: 4641–4647.
20. Leisner TM, Wencel-Drake JD, Wang W, et al. Bidirectional transmembrane modulation of integrin $\alpha_{IIb}\beta_3$ conformations. J Biol Chem 1999; 274: 12945–12949.
21. Haas TA, Plow EF. Development of a structural model for the cytoplasmic domain of an integrin. Protein Eng 1997; 10: 1395–1405.
22. Vallar L, Melchior C, Plancon S, et al. Divalent cations differentially regulate integrin a_{IIb} cytoplasmic tail binding to β_3 and to calcium- and integrin-binding protein. J Biol Chem 1999; 274: 17257–17266.
23. Haas TA, Plow EF. The cytoplasmic domain of $\alpha_{IIb}\beta_3$: a ternary complex of the integrin α and β subunits and a divalent cation. J Biol Chem 1996; 271: 6017–6026.
24. Vinogradova O, Haas TA, Plow EF, et al. A structural basis for integrin activation by the cytoplasmic tail of the a_{IIb}-subunit. Proc Natl Acad Sci USA 2000; 97: 1450–1455.
25. Vinogradova O, Velyvis A, Velyviene A, et al. A structural mechanism of integrin αIIbβ3 'inside-out' activation as regulated by its cytoplasmic face. Cell 2002; 110: 587–597.
26. Otey CA, Pavalko FM, Burridge K. An interaction between α-actin and the β_1 integrin subunit in vitro. J Cell Biol 1990; 111: 721–729.
27. Obergfell A, Eto K, Mocsai A, et al. Coordinate interactions of Csk, Src, and Syk kinases with $\alpha_{IIb}\beta_3$ initiate integrin signaling to the cytoskeleton. J Cell Biol 2002; 157: 265–275.
28. Calderwood DA, Zent R, Grant R, et al. The talin head domain binds to integrin b subunit cytoplasmic tails and regulates integrin activation. J Biol Chem 1999; 274: 28071–28074.
29. Shattil SJ, O'Toole TE, Eigenthaler M, et al. β_3-Endonexin, a novel polypeptide that interacts specifically with the cytoplasmic tail of the integrin β_3 subunit. J Cell Biol 1995; 131: 807–816.
30. Reddy KB, Gascard P, Price MG, et al. Identification of an interaction between the M-band protein Skelemin and beta -integrin subunits. Colocalization of a Skelemin-like protein with beta 1– and beta 3-integrins in non-muscle cells. J Biol Chem 1998; 273: 35039–35047.
31. Kieffer JD, Plopper G, Ingber DE, et al. Direct binding of F actin to the cytoplasmic domain of the a2 integrin chain in vitro. Biochem Biophys Res Commun 1995; 217: 466–474.
32. Knezevic I, Leisner TM, Lam SCT. Direct binding of the platelet integrin $\alpha_{IIb}\beta_3$ (GPIIb- IIIa) to talin. Evidence that interaction is mediated through the cytoplasmic domains of both α_{IIb} and β_3. J Biol Chem 1996; 271: 16416–16421.
33. Naik UP, Patel PM, Parise LV. Identification of a novel calcium-binding protein that interacts with the integrin a_{IIb} cytoplasmic domain. J Biol Chem 1997; 272: 4651–4654.
34. Kato A, Kawamata N, Tamayose K, et al. Ancient ubiquitous protein 1 binds to the conserved membrane-proximal sequence of the cytoplasmic tail of the integrin α subunits that plays a crucial role in the inside-out signaling of $\alpha_{IIb}\beta_3$. J Biol Chem 2002; 277: 28934–28941.
35. Larkin D, Murphy D, Reilly DF, et al. ICln, a novel integrin αIIbβ3-associated protein, functionally regulates platelet activation. J Biol Chem 2004; 279: 27286–27293.
36. Vijayan KV, Liu Y, Li TT, et al. Protein phosphatase 1 associates with the integrin aIIb subunit and regulates signaling. J Biol Chem 2004; 279: 33039–33042.
37. Yuan W, Leisner TM, McFadden AW, et al. CIB1 is an endogenous inhibitor of agonist-induced integrin αIIbb3 activation. J Cell Biol 2006; 172: 169–175.

38. Stephens G, O'Luanaigh N, Reilly D, et al. A sequence within the cytoplasmic tail of αIIb independently activates platelet aggregation and thromboxane synthesis. J Biol Chem 1998; 273: 20317–20322.
39. Aylward K, Meade G, Ahrens I, et al. A novel functional role for the highly conserved a-subunit KVGFFKR motif distinct from integrin αIIbβ3 activation processes. J Thromb Haemost 2006; 4: 1804–12–1812.
40. Barry WT, Boudignon-Proudhon C, Shock DD, et al. Molecular basis of CIB binding to the integrin α_{IIb} cytoplasmic domain. J Biol Chem 2002; 277: 28877–28883.
41. Ginsberg MH, Yaspan B, Forsyth J, et al. A membrane-distal segment of the integrin a_{IIb} cytoplasmic domain regulates integrin activation. J Biol Chem 2001; 276: 22514–22521.
42. Plow EF, Srouji AH, Meyer D, et al. Evidence that three adhesive proteins interact with common recognition site on activated platelets. J Biol Chem 1984; 259: 5388–5391.
43. Yan B, Calderwood DA, Yaspan B, et al. Calpain cleavage promotes talin binding to the b_3 integrin cytoplasmic domain. J Biol Chem 2001; 276: 28164–28170.
44. D'Souza SE, Haas TA, Piotrowicz RS, et al. Ligand and cation binding are dual functions of a discrete segment of the integrin b_3 subunit: cation displacement is involved in ligand binding. Cell 1994; 79: 659–667.
45. Porte F, Liautard J.-P, Köhler S. Early acidification of phagosomes containing *Brucella suis* is essential for intracellular survival in murine macrophages. Infect Immun 1999; 67: 4041–4047.
46. Patil S, Jedsadayanmata A, Wencel-Drake JD, et al. Identification of a talin-binding site in the integrin b_3 subunit distinct from the NPLY regulatory motif of post-ligand binding functions. The talin n-terminal head domain interacts with the membrane-proximal region of the b_3 cytoplasmic tail. J Biol Chem 1999; 274: 28575–28583.
47. Schlaepfer DD, Hunter T. Focal Adhesion Kinase Overexpression Enhances Ras-dependent Integrin Signaling to ERK2/Mitogen-activated Protein Kinase through Interactions with and Activation of c-Src. J Biol Chem 1997; 272: 13189–13195.